



## Controlling the phase morphology of immiscible poly(2,6-dimethyl-1,4-phenylene ether)/poly(styrene-co-acrylonitrile) blends via addition of polystyrene

Andreas Göldel,<sup>1,3</sup> Holger Ruckdäschel,<sup>1</sup> Axel H.E. Müller,<sup>2</sup> Petra Pötschke,<sup>3</sup> Volker Altstädt<sup>1\*</sup>

<sup>1</sup>\* Department of Polymer Engineering, University of Bayreuth, Universitätsstrasse 30, 95447 Bayreuth, Germany; fax: +49 (0) 921 - 55 7473; e-mail: altstaedt@uni-bayreuth.de

<sup>2</sup> Department of Macromolecular Chemistry II, University of Bayreuth, Universitätssstrasse 30, 95447 Bayreuth, Germany; fax: +49 (0) 921 - 55 7473; e-mail: axel.mueller@uni-bayreuth.de

<sup>3</sup> Department of Polymer Reactions and Blends, Leibniz Institute of Polymer Research Dresden e.V. (IPF), Hohe Strasse 6, 01069 Dresden, Germany

(Received: 20 November, 2007; published: 24 November, 2008)

**Abstract:** The microstructure of melt-processed, immiscible poly(2,6-dimethyl-1,4-phenylene ether)/poly(styrene-co-acrylonitrile) blends (PPE/SAN) was controlled by systematically adjusting the viscosity ratio between both phases. For this purpose, low-viscous polystyrene (PS) was added as a third component, as it shows selective miscibility with PPE and thus allows the varying of the shear viscosity of PPE over a broad range. In order to theoretically predict the phase morphology, a model following Utracki was applied taking into account the viscosity ratio and the respective volume contents of each phase. Detailed transmission electron microscopic investigations of the blend morphologies demonstrated excellent agreement with theory. Moreover, quantitative evaluation of the observed microstructures allowed further description of the degree of blend co-continuity. Thus, desirable compositions of the ternary blend systems could be identified which potentially show enhanced properties such as a high heat deflection temperature, an elevated strength, stiffness, and ease of processing. Finally, a optimum (PPE/PS)/SAN blend system that has been optimised regarding the aforementioned properties was compatibilized by polystyrene-b-poly(1,4-butadiene)-b-poly(methyl methacrylate) triblock terpolymers. Due to the interfacial enrichment of the block copolymer, nanostructured blend morphologies were observed. In the view of these results, pathways to control both the micro- and the nanostructure of PPE/SAN blends are derived, potentially useful to enhance the mechanical as well as thermo-mechanical property profile.

### Introduction

Blending of polymers provides an efficient route to develop new materials with tailored properties [1, 2]. Using an already existing range of base polymers, a large variety of new high-performance polymer blends is readily and economically available. In particular, immiscible blends of poly(2,6-dimethyl-1,4-phenylene ether) (PPE) and poly(styrene-co-acrylonitrile) (PPE/SAN) are expected to provide various advantages by combining the toughness, the flame-retardant behaviour, and the high heat distor-

tion temperature of PPE with the chemical resistance, the high stiffness, the resistance to stress cracking and the low material costs of SAN.

Recently, the phase morphology and the property profile of melt-processed PPE/SAN blends were extensively investigated by Ruckdäschel et al. [3, 4]. As PPE and SAN show immiscibility over the complete composition range, the studies were focused on the compatibilization step by various polystyrene-*b*-poly(1,4-butadiene)-*b*-poly(methyl methacrylate) triblock terpolymers (SBM). As could be shown, such SBM triblock terpolymers locate at the interface when appropriately composed. Furthermore, the compatibilization leads to the development of a specific nanostructure, also referred to as "raspberry morphology" [3-5]. This peculiar phase morphology was identified as a key factor for significantly enhancing the blend toughness, while keeping the strength as well as the modulus at a rather high level [4].

For achieving enhanced macroscopic properties such as impact toughness and elevated heat deflection temperatures, not only the nanostructure but also the microstructure of the blend needs to be controlled. For the present blend system, a high degree of continuity of both PPE and SAN appears desirable, in order to benefit the property profile of both phases. However, up to PPE contents of 60 wt%, melt-processed PPE/SAN blends show a more continuous SAN phase so far, while the PPE appears to be rather dispersed. Thus, the blend reveals rather poor thermo-mechanical properties. In order to overcome this limitation, the formation of co-continuous structures appears desirable. These co-continuous blends are expected to offer a synergistic property profile compared to the individual blend partners, therefore numerous investigations were focused on their formation [6-18, 31] and their properties [19-23].

As the phase morphology development of immiscible polymer blends during twin-screw-extrusion is influenced by the processing conditions and by numerous physical properties of the blend system, the prediction of the final microstructure is rather complex. Due to the deformation, break-up and coalescence of all phases in presence of shear and elongational flow, various, rather complex shapes are typically observed. As a result, a general as well as reliable simulation and thus precise prediction of the final blend phase morphology following twin-screw extrusion therefore still remains a challenge [24]. However, the superior importance of viscosity ratio and the blend composition on phase morphology development has been reported in numerous publications [7, 25-27].

In view of the discussed PPE/SAN 60/40 blend system, the significantly higher viscosity of PPE, compared to SAN, strongly hinders the formation of co-continuous phase morphologies. In order to overcome this disadvantage and to develop co-continuous blends, three promising approaches can be deduced from literature: (i) increasing the PPE content beyond 60 wt%, (ii) increasing the viscosity of the SAN phase and (iii) reducing the viscosity of the PPE phase.

With regard to the first two approaches, significantly increased melt temperatures, typically in the range of 300 °C, are needed to process the material. In turn, severe thermal degradation of PPE and SAN would result. Moreover, the thermal stability of SBM triblock terpolymers, which are foreseen to compatibilise the blend systems, would severely degrade and decompose under such temperatures [3]. Therefore, both the use of elevated PPE contents as well as the selection of higher-viscous SAN grades is limited. It therefore appears more advantageous to reduce the viscosity of PPE.

The selection of lower molecular weight PPE could help to reduce the viscosity; however, a significant reduction of the chain length of PPE also detrimentally affects the materials performance, particularly regarding the toughness and the chemical resistance. Tailoring of the viscosity ratio by the addition of a third, low-viscous component which shows miscibility with PPE, but immiscibility with SAN therefore appears to be more promising.

For this purpose, polystyrene (PS) can be regarded as material of choice, as it shows miscibility with PPE over the complete compositional and temperature range. In addition, synergisms in tensile strength, tensile modulus and physical behaviour have been reported for blends of PPE and PS [29, 30].

The potential of selective blending of immiscible blends composed of PPE and another polymer with PS has been reported for other blend systems [26, 27]. In these studies, the homogeneous miscibility of PPE/PS was exploited to systematically vary the viscosity ratio of (PPE/PS)/PP [26], and (PPE/PS)/PA6 blends [27]. Thus, the phase morphology of such systems could be controlled via the viscosity ratio, while only minor changes of the interfacial tension are observed [31].

The aim of the present study is to systematically control the phase morphology development of immiscible PPE/SAN blends via selective blending with PS, in order to finally achieve co-continuous blend systems. The morphology development, as investigated by transmission electron microscopy, is compared to theoretical models predicting the phase inversion as a function of viscosity and blend composition. In this context, shear rheological measurements are performed in order to investigate the correlation between theoretical predictions and the blend morphologies. Finally, ternary blends compatibilized by triblock terpolymers are developed, aiming at controlling both the micro- and the nanostructure for further enhancing the property profile of the blend system, particularly regarding the toughness.

It should be noted that the current study only aims at providing a basic understanding of the phase morphology development, while its correlation with the overall property profile of the blends will be presented in an upcoming publication. There, we will particularly focus on the effect of adding PS to PPE/SAN blends, at first view deterioration of the blend performance due to the embrittlement and reduction in glass transition temperature of the PPE phase. Nevertheless, we will demonstrate that synergisms in blend behaviour are observed when carefully controlling both the micro- and the nanostructure.

## Results

### *Blending strategy*

In a first step, the blending strategy as well as the subsequent selection of the respective compositions will be described. As aforementioned, recent results on PPE/SAN 60/40 (wt/wt) blends revealed a SAN matrix, as a result of the extrusion process. The viscosity of the high-viscous PPE phase, as one of the main factors controlling the blend morphology, should therefore be systematically reduced, while the SAN content was fixed at 40 wt%. Such behaviour should be adjusted by an increasing content of low-viscous PS and the subsequent reduction of the PPE content. The resulting blend compositions are shown in Fig. 1 (full symbols).

In order to allow the direct comparison of the viscosity ratio between PPE/PS and SAN with different theoretical models, describing the morphology development in

two-phase (PPE/PS)/SAN blends, the rheological properties of the three different binary PPE/PS blends (Fig. 1, open symbols) as well as SAN were investigated.

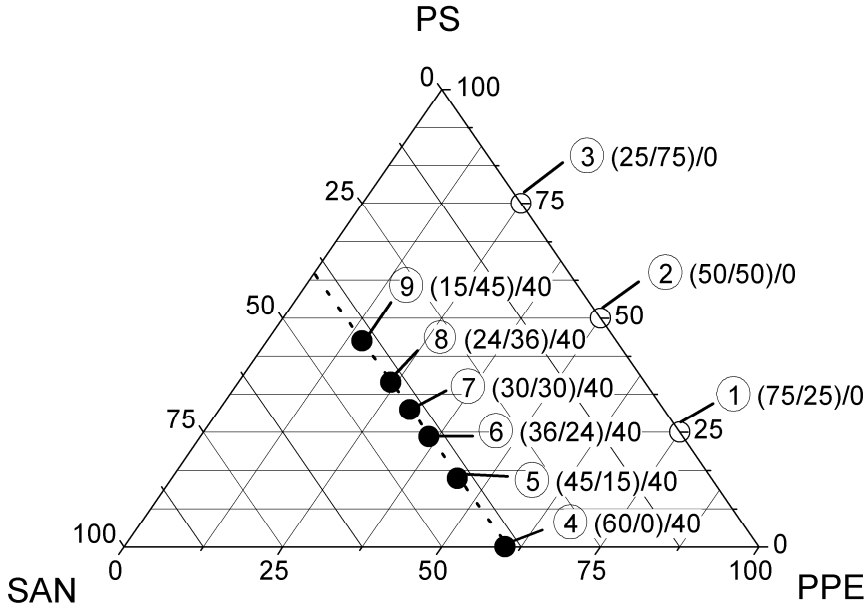


**Fig. 1.** Blending strategy to control the microstructure of PPE/SAN blends. Compositions of the investigated binary PPE/PS (open symbols) and ternary (PPE/PS)/SAN blend systems (full symbol). Numbers indicate the composition in wt% and the number of the blend system, respectively (see also Table 1).

#### Rheological properties and prediction of the phase inversion

The rheological properties of the neat polymers PS, PPE and SAN at 260 °C are shown in Fig. 2a, as observed by oscillatory plate-plate rheometry. It should be noted that the shear-rate dependent complex viscosity was calculated based on the experimental data using Eq. 1 [32]:

$$|\eta^*| = \frac{1}{\omega} \sqrt{G'^2 + G''^2} \quad (1)$$

where  $G'$  and  $G''$  denote the storage and the loss modulus, respectively. The storage modulus quantifies the immediate response of a polymer towards the forced shear deformation, and thus describes the energy stored and subsequently released within one oscillation cycle. In contrast, the loss modulus relates to the energy lost within the polymer melt due to friction phenomena. Returning to Fig. 2a, it can be seen that the viscosity of PPE is significantly higher compared to SAN, while PS reveals a much lower viscosity. Due to their miscibility, it can be anticipated that the selected PPE/PS blends can cover the viscosity regime between the two extremes, PPE and PS, and can show similar viscosities as SAN. Indeed, the results outlined in Fig. 2b verify such a behaviour, in accordance to literature [2].

In order to relate the complex viscosity, observed by oscillatory shear measurements, with the shear viscosity as a function of shear rate, the Cox-Merz rule was applied (Eq. 2):

$$\eta(\dot{\gamma}) = |\eta^*(\omega)| \text{ at } \dot{\gamma} = \omega \quad (2)$$

As the shear rate regime typically observed during twin-screw-extrusion ranges from 1–1,000 s<sup>-1</sup> [32], the presented rheological data can almost completely cover the regime relevant for processing. The viscosity behaviour of SAN and of PPE and its blends with PS will subsequently be exploited to theoretically predict the phase morphology of ternary (PPE/PS)/SAN blends.

As one of the crucial factors for the morphology development, the shear rate-dependent viscosity ratio,  $p_{\text{eff}}$ , can be calculated as ratio between the melt viscosities of the dispersed phase,  $\eta_d(\dot{\gamma})$ , and the matrix phase,  $\eta_m(\dot{\gamma})$ , respectively (Eq. 3):

$$p_{\text{eff}}(\dot{\gamma}) = \frac{\eta_d(\dot{\gamma})}{\eta_m(\dot{\gamma})} \quad (3)$$

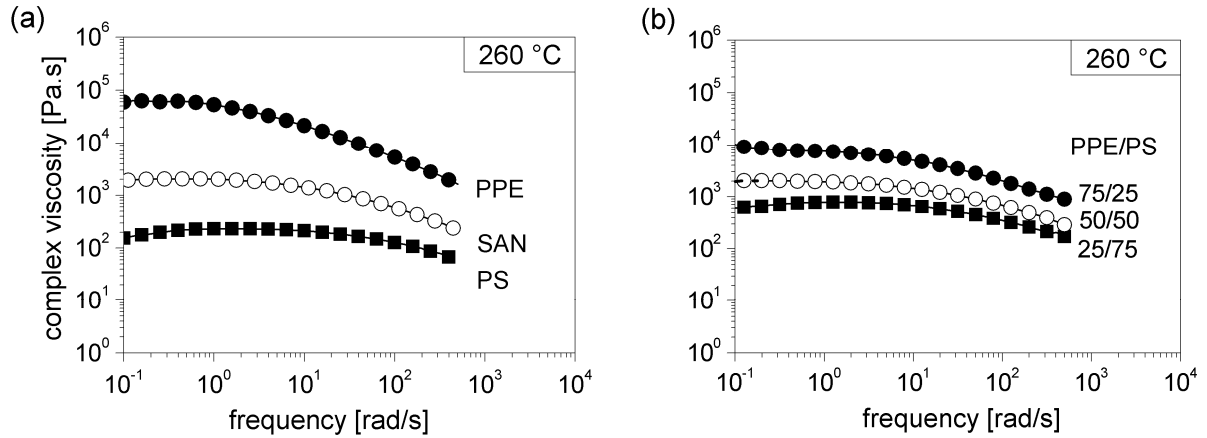


**Fig. 2.** Rheological behaviour of the investigated reference systems at 260 °C. (a) Neat polymers. (b) Miscible PPE/PS blends.

The resulting viscosity ratio of (PPE/PS)/SAN blends at 260 °C is shown in Fig. 3. It should be noted that PPE/PS is regarded as the dispersed blend phase for these considerations. As can be seen, the viscosity ratio of the high viscous PPE-phase and SAN is higher than 10, while a value well below one is observed for the blend pair PS and SAN. In addition, the shear rate dependence of the viscosity ratio can be clearly seen, an effect that can show strong impact on the morphology development at different processing conditions. Interestingly, PPE/PS 50/50 blends show similar viscosities as SAN over the complete investigated shear rate regime. Two particular models are described in the following, correlating the viscosity ratio and the phase inversion composition. When discussing the phase morphology development of immiscible blends, it appears to be obvious that the low-viscosity blend phase tends to form matrix phase in a polymer blend. A first model to establish a link between the viscosity ratio and the blend composition with the blend morphology was proposed by Miles and Zureck (Eq. 4) [33]:

$$\frac{\eta_1(\dot{\gamma})}{\eta_2(\dot{\gamma})} = \frac{\Phi_{1I}}{\Phi_{2I}} \quad (4)$$

Here, the parameters  $\eta_1$  and  $\eta_2$  denote the viscosity of the two phases, while  $\phi_1$  and  $\phi_2$  indicate the respective volume contents at phase inversion. In the present case, SAN forms the first phase, while the second phase is composed of PPE and its blends with PS. The simplicity of the model allows to easily estimate the phase inver-

sion of blend system; however, it is only valid for viscosity ratios close to unity and at low shear rates, thus limiting its use.

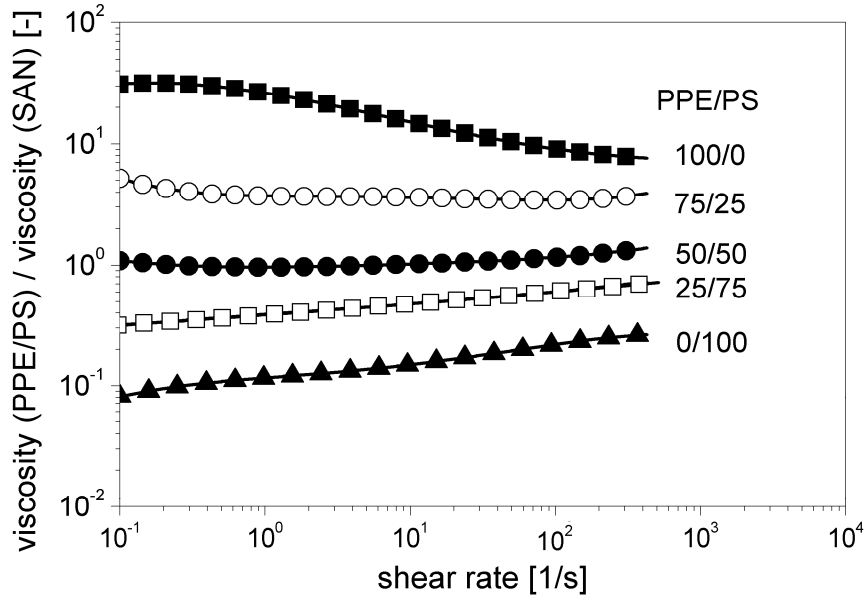


**Fig. 3.** Viscosity ratio between PPE, PS and its blends versus SAN as a function of shear rate at 260 °C.

In order to overcome this disadvantage, an alternative model was proposed by Utracki [34], which can also be applied for high viscosity ratios:

$$\phi_2 = \frac{\phi_m + (1 - \phi_m) \cdot p^{\left(\frac{1}{[\eta]\Phi_1}\right)}}{p^{\left(\frac{1}{[\eta]\Phi_1}\right)} + 1} \quad (5)$$

where  $\phi_2$  denotes the volume content of the second phase when phase inversion occurs. The parameters  $\phi_m$  and  $[\eta]$  indicate the maximum packing density of spheres in vol% and the intrinsic viscosity, respectively. It should be noted that  $\phi_m$  is linked to the percolation threshold for a dispersion of spheres ( $\phi_m = 1 - \phi_c$ ). In the present case, parameters were taken from literature to predict the phase morphology ( $\phi_m = 0.16$  and  $[\eta] = 1.9$ ) [34]. As demonstrated, the theoretical predictions by the Utracki equation show good agreement with the observed morphologies of numerous blend systems.

It has to be stated that the present work correlates the melt-volume based theoretical predictions and the mass-related blend compositions. This simplification was based on the negligible density differences of the amorphous polymers PPE, PPE/PS and SAN at room temperature. Generally PPE, PS and their binary blends show densities between 1.04 g/cm<sup>3</sup> and 1.07 g/cm<sup>3</sup> with a maximum value at the synergistic composition of PPE<sub>75</sub>/PS<sub>25</sub>, in comparison to a SAN-value of 1.07 g/cm<sup>3</sup>. Therefore the calculation of phase-inversion volume contents was done assuming similar melt densities in the different blend phases.

In the particular case of PPE/SAN 60/40 blends, the high viscosity ratio between the two phases indeed can be identified as primary reason for the low continuity of the PPE phase, independent of the model used.

In Figure 4, the theoretical prediction of the blend morphology is combined with the rheological measurements of SAN and PPE/PS blends, for estimating the phase inversion concentration by the Utracki model. In order to relate the compositional range of phase inversion to the investigated blend systems, a dashed line is added for a fixed SAN content of 40 vol%. Blend systems close to this line are predicted to show co-continuous phase morphologies. It can be clearly seen that neat PPE/SAN blends require minimum PPE contents of 70 vol% in order to ensure phase inversion. In contrast, the addition of only 15 wt% of PS significantly reduces this minimum content, revealing 62 vol% of the PPE/PS phase to observe complete co-continuity. Thus, a significant degree of co-continuity can be expected for a (PPE/PS)/SAN blend system. Further increasing the PS-content is expected to lead to phase-inversion, where SAN is finally dispersed in a PPE/PS matrix.

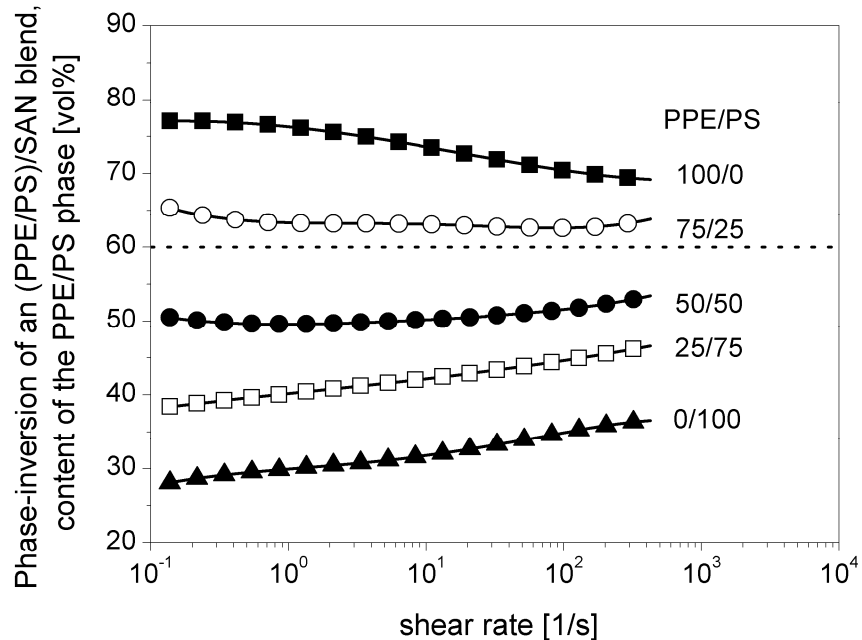


**Fig. 4.** Utracki model: prediction of the phase-inversion concentration in blends of (PPE/PS)/SAN for different compositions of the PPE/PS phase as a function of shear rate. The line indicates the selected content of PPE/PS in the ternary (PPE/PS)/SAN blends of this study.

#### *Development and control of the microstructure*

As aforementioned, the morphological structure in immiscible blends is strongly related to the rheological properties of the blend components. For PPE/SAN blends (Fig. 5a), the high viscosity ratio ( $\rho = \eta_{\text{PPE}}/\eta_{\text{SAN}}$ ) can be identified as the main reason for the formation of a SAN matrix during extrusion, even for PPE contents of 60 wt%. It is worth noting that the PPE phase appears not fully dispersed, but reveals rather complex shapes and sub-inclusions of SAN, which indicates a certain degree of continuity. However, a PPE matrix or ideally co-continuous morphologies would be preferred.

Besides the empirical models describing the parameter needed to ensure the desired phase inversion, Sundararaj et al. [35] proposed a descriptive model for understanding the general mechanisms occurring during melt mixing and phase morphology development. Adapting the model to the PPE/SAN blend, the lower melting temperature

of SAN (glass transition temperature of 114 °C) will lead to a continuous phase of molten SAN with dispersed, solid PPE particles (glass transition temperature of 216 °C) during the initial phase of extrusion. After softening of the disperse PPE particles, the blend morphology is determined by a dynamic interaction of droplet break-up and coalescence processes [36]. Dominating coalescence of the previously dispersed PPE phase can lead to subsequent phase inversion. Here, low viscosities and high contents of the PPE phase would promote the phase inversion.

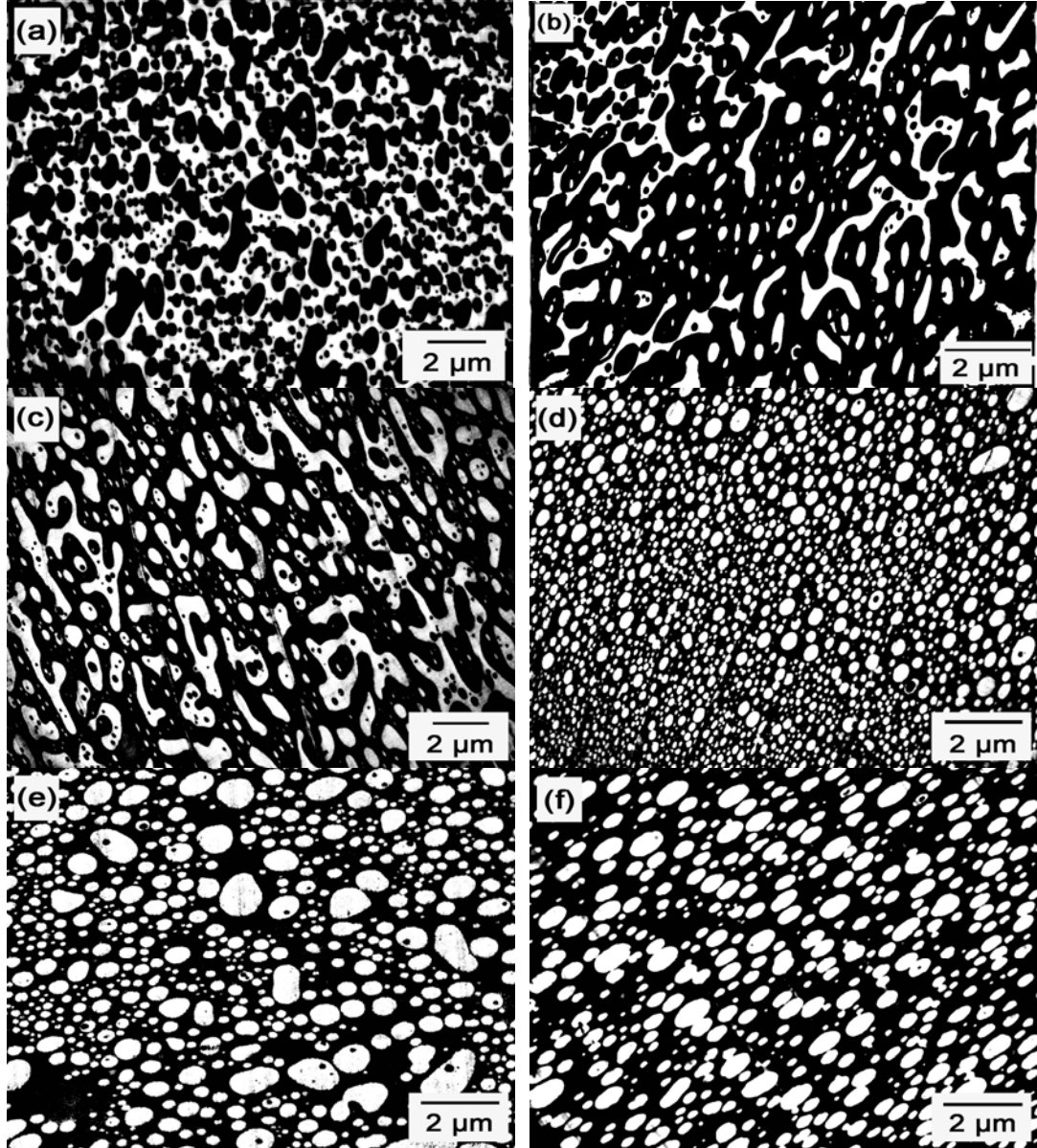


**Fig. 5.** Phase morphology of extruded (PPE/PS)/SAN blends as observed by transmission electron microscopy. (a) PPE/SAN 60/40. (b) (PPE/PS)/SAN (45/15)/40. (c) (PPE/PS)/SAN (36/24)/40. (d) (PPE/PS)/SAN (30/30)/40. (e) (PPE/PS)/SAN (24/36)/40. (f) (PPE/PS)/SAN (15/45)/40. The micrographs were transferred to black-and-white images to allow computer-aided evaluation of the blend morphology. The black phase indicates the PPE/PS phase, while the white phase denotes the SAN phase.

As shown in the previous section, the selective blending of PPE/SAN blends with PS allows to reduce and to even control the viscosity ratio of the two-phase

(PPE/PS)/SAN blend, which is expected to result in an increased continuity of the PPE/PS phase.

The phase morphology of all investigated (PPE/PS)/SAN blends is shown in Fig. 5. It should be noted that the structure was observed by transmission electron microscopic investigations of the melt strands cut in perpendicular to the extrusion direction. As can be seen, the addition of only 15 wt% of PS causes a significant change in blend morphology (Fig. 5b). The starting phase inversion leads to a blend morphology containing an almost equal amount of the three relevant morphologies - particularly areas containing mainly SAN-matrix, but also those with PPE/PS-matrix and rather complex co-continuous regions. More precisely, fine-dispersed inclusions of SAN are observed within an elongated PPE/PS phase. All these features can be accessed in Fig. 5b: starting from the upper left corner, a transition of the neat SAN-matrix into a complex PPE/PS matrix structure is visible and, finally, the development towards a co-continuous structure demonstrated in the lower right corner. Such morphological features clearly indicate the compositional range, where phase inversion takes place.

In order to quantitatively describe the co-continuous characteristics, the method of selective solvent extraction of the less continuous phase is often performed [18]. Unfortunately, no selective solvent systems is available for the present (PPE/PS)/SAN blend. Therefore, the TEM micrographs were further analysed. Here, the so-called form factor of the individual particles,  $F$ , was recently identified as a measure for the co-continuity [38]:

$$F = 4\pi \frac{A}{P^2} \quad (6)$$

where  $A$  and  $P$  denote the area and the perimeter of one particle. In the case of a fully dispersed, spherical PPE phase, the form factor approaches unity, whereas lower values can be anticipated for irregularly shaped domains, which are associated with an increasing continuity of the blend. In order to correctly describe the blend morphology with a single value, a co-continuity parameter,  $C$ , calculated as an area-averaged form factor, is introduced for the present blend systems [15]:

$$C = 1 - \frac{\sum_i A_i F_i}{\sum_i A_i} \quad (7)$$

For complete co-continuity, the value approaches values up to one, while lower values indicate lower continuity of the dispersed phase. For completely spherical, fully dispersed phases in a matrix, a value of zero will be observed.

The results for (PPE/PS)/SAN blend are shown in Fig. 6, verifying the qualitative descriptions of the TEM micrographs. Starting with the PPE/SAN 60/40 blend, a certain degree of continuity of the dispersed PPE phase can be detected. Moreover, the addition of low contents of PS leads to rather co-continuous blend systems of (PPE/PS)/SAN (45/15)/40. In such a blend, the PPE content of the PPE/PS phase is still remarkably high (75 wt%), potentially providing high heat deflection temperatures and toughness and furthermore corresponding with the maximum synergism in modulus and tensile strength in the PPE/PS phase. By the further addition of PS, the continuity of SAN is stepwise reduced, while PPE/PS forms the matrix. It should be noted that the value of zero is not approached, still indicating some continuity of the SAN phase. Such observations are in accordance with the general behaviour of

blends at such high contents of the dispersed phase (as 40 wt% in the present case), as highlighted by Utracki [2].

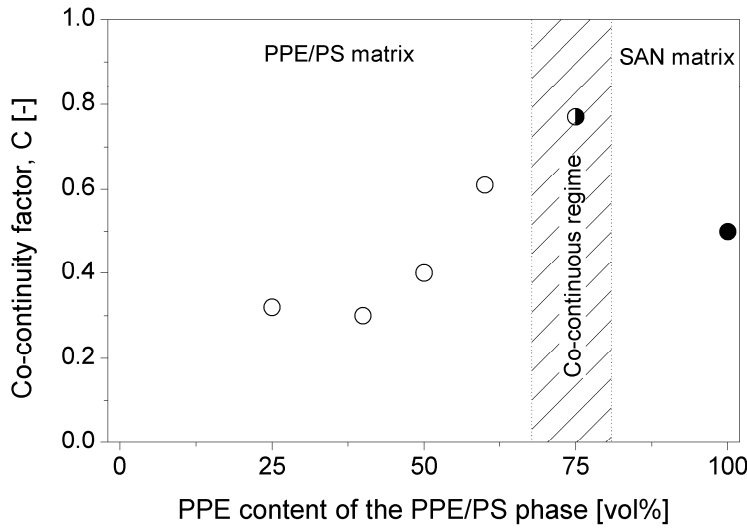


**Fig. 6.** Co-continuity of (PPE/PS)/SAN blends at a fixed SAN content of 40 wt%. The co-continuity factor, as calculated according to Eq. 7, allows to quantitatively accessing the microstructure of the blend (full symbols indicate a PPE/PS matrix, open symbols indicate an SAN matrix; half symbols are used for co-continuous systems). Details on the blend compositions can be found in Table 1.

For such a complex blend system as (PPE/PS)/SAN, consisting of three components, a reliable prediction of the phase morphology over the complete compositional range would be very valuable. For this purpose, the Utracki model was applied to predict the phase inversion for blends at different shear rates of  $1\text{-}100 \text{ s}^{-1}$ , typically observed during extrusion. The values are subsequently plotted in a ternary phase diagram of PPE, PS and SAN, allowing access of the blend structure as well as its shear rate dependence. As previously shown, an increase in PS content lead to a reduction of the PPE/PS amount, which is predicted to be necessary for the observation of phase-inversion.

As an example, the model proposes for PPE/SAN blends a PPE content of 70.4 vol% ( $100 \text{ s}^{-1}$ ) and 76 vol% ( $1 \text{ s}^{-1}$ ) for phase-inversion, highlighting its dependence on shear rate. Here, higher shear rates promote the formation of an SAN matrix. As further example, for (PPE/PS)/SAN-blends containing a PPE/PS phase composed of 25 wt% PPE and 75 wt% PS, phase-inversion can be expected for 44 vol% of (PPE/PS) at a shear rate of  $100 \text{ s}^{-1}$ , while slightly lower contents of 40 vol% are needed at reduced shear rates of  $1 \text{ s}^{-1}$ . Such a shear rate dependence of the phase-inversion concentration is the result of the different shear-thinning behaviour of the PPE/PS blends and SAN (see also Fig. 2). Besides the extrusion process, the structure formation during injection-moulding, employing even higher shear rates in the range of  $1,000\text{-}10,000 \text{ s}^{-1}$  will be discussed in following publications.

Returning to Fig. 7, the lines indicating the predicted phase inversion compositions according to the Utracki model separate the ternary phase diagram in two regimes, where either a PPE/PS matrix or a SAN matrix is observed. As can be seen for the investigated blend system, the line is approximately crossed by the (PPE/PS)/SAN 45/15/40 blend, in accordance with the aforementioned results.

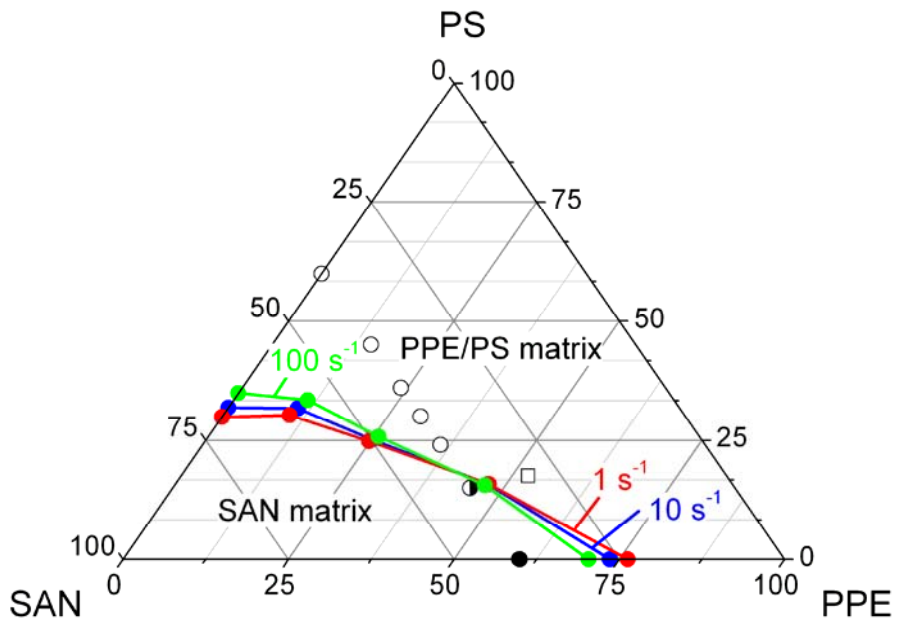


**Fig. 7.** Ternary phase diagram of the (PPE/PS)/SAN blend system showing the shear rate dependent phase inversion compositions (coloured symbols, lines are drawn to guide the eye) and the investigated blend systems (open circles: PPE/PS matrix; half circles: co-continuity; full circles: SAN matrix). In addition, the blend system used for compatibilization with SBM is shown (open square).

All investigated blend systems were composed of 40 wt% of SAN and 60 wt% of PPE/PS so far, aiming at a suitable balance of processability and toughness. Furthermore taking into account the synergism between PPE and PS in strength [29] and modulus [30], but also in charge storage behaviour [28], blends with a PPE/PS ratio of 75/25 appear as the most promising candidate. However, as highlighted by Fig. 7, the particular blend system coming into question, the (PPE/PS)/SAN (45/15)/40 blend, is rather close to phase inversion. As a continuous PPE/PS phase needs to be ensured after extrusion as well as following an injection moulding process, it appears reasonable to further increase the PPE/PS content of the blend to a minor extent.

In addition, one further aspect promotes such a proceeding: The shear rate observed during injection-moulding is typically rather high and, as can be seen in Fig. 7, increasing shear rates lead to a shift of phase inversion towards elevated PPE/PS contents. Therefore an optimised ternary (PPE/PS)/SAN blend was compounded (Fig. 8) ensuring both an optimum composition within the PPE/PS phase and an increased total PPE/PS content of 70 wt%. In contrast to two-component PPE/SAN blends, such blends can be easily processed at relatively low contents of SAN, due to the reduced viscosity within the PPE phase. As expected, Fig. 8 reveals a stable continuous PPE/PS phase, which is assumed to provide a high heat deflection temperature and enhanced mechanical properties of the blend. In addition, the still remarkably high degree of continuity of SAN also promises to take advantage of the properties of SAN such as the enhanced chemical resistance and ease of processing. Furthermore, the formation of very fine droplet-in-droplet structures is observed, a phenomenon reported for several blend systems in the phase-inversion region [24, 26].

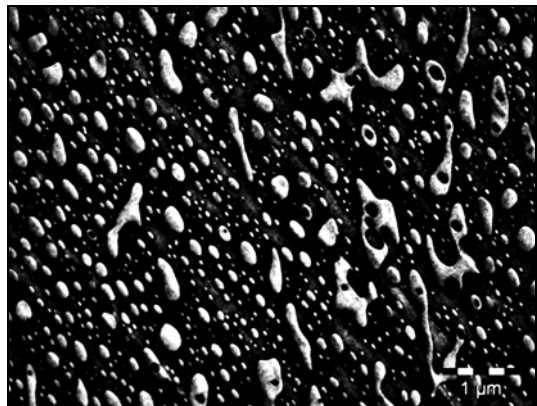


**Fig. 8.** Phase morphology of an optimised ternary (PPE/PS)/SAN (52.5/17.5)/30 blend (Blend No. 10, dark phase: PPE/PS, bright phase: SAN).

#### *Development and control of the micro- and nanostructure*

Based on the successful development of (PPE/PS)/SAN blends, showing the desired microstructure, the subsequent compatibilization by the addition of 10 wt% of polystyrene-b-polybutadiene-b-poly(methyl methacrylate) triblock terpolymers (SBM) was investigated. Compatibilization is an efficient and well-accepted method to improve the interfacial strength between the components in a two-phase blend, hence enhancing the mechanical properties of the blend. In addition, the interfacial tension and the coalescence between the blend partners, that is determined by their surface tensions and polarities [40], is decreased, effects that lead to a finer and more stable morphology [39], which also is beneficial for the overall mechanical performance [1].

Block copolymers, in particular, are commonly used to improve the adhesion of immiscible blend components due to a selective miscibility of the blocks with either blend component. The use of polystyrene-b-polybutadiene-b-poly(methyl methacrylate) (SBM) triblock terpolymers in immiscible PPE/SAN blends can be regarded as a particular compatibilization strategy for observing nanostructured blends, as demonstrated in the pioneering work of Stadler et al. [5] for solvent-mediated processing and more recently by Ruckdäschel et al. [3] for melt-processing. Each end block of the SBM is selectively miscible with one blend component, in particular, an entanglement of PMMA in SAN (miscibility for AN content of 19 wt%) and of PS in PPE is observed. The incompatibility of the elastomeric middle block with both the blend components and the end blocks as well as the balanced chemical interaction parameters lead to a discontinuous and nanoscale distribution of PB spheres within the interface. It is this nanostructured morphology, also referred to as ‘raspberry morphology’, which allows toughening of PPE/SAN blends at a minimum decrease in both stiffness and strength [4, 5].

As demonstrated by Ruckdäschel et al. [3,4], SBM triblock terpolymers with similar weight contents of each block and sufficiently high block lengths allow both the formation of nanostructures as well as toughening of PPE/SAN blends. In this study, two different processing approaches to compatibilize the optimized blend system (Blend No. 10, Fig. 8) were investigated: (i) all four components were added simultaneously into the twin-screw extruder (Fig. 9a) and (ii) first, the ternary (PPE/PS)/SAN

blends was prepared and, as a second step, the pellets were compatibilized by SBM by an additional compounding step (Fig. 9b).

Comparing the one-step and the two-step processing, distinct differences in both micro- and nanostructure are observed. As can be seen from Fig. 9a, simultaneous compounding of all four components leads to an unfavourable distribution of the SBM triblock terpolymers, as the interphase is only partially covered and micelle formation can be detected. However, in the case of the two-step approach, this procedure ensured the desired nanostructure formation by the interfacial presence of SBM (Fig. 9b). Moreover, a continuous PPE/PS phase is formed. Here, the complexity of the quaternary blend system demands for a pre-blending of PPE, PS and SAN.

In summary, the outlined approaches describe, how both the micro- as well as the nanostructure of PPE/SAN blends can be controlled via aimed addition of PS and of SBM triblock terpolymers. Regarding the toughness and the thermo-mechanical behaviour, an excellent property profile of such quaternary blends is expected. A detailed study of the processing behaviour and the mechanical properties will be focused on in the next paper.

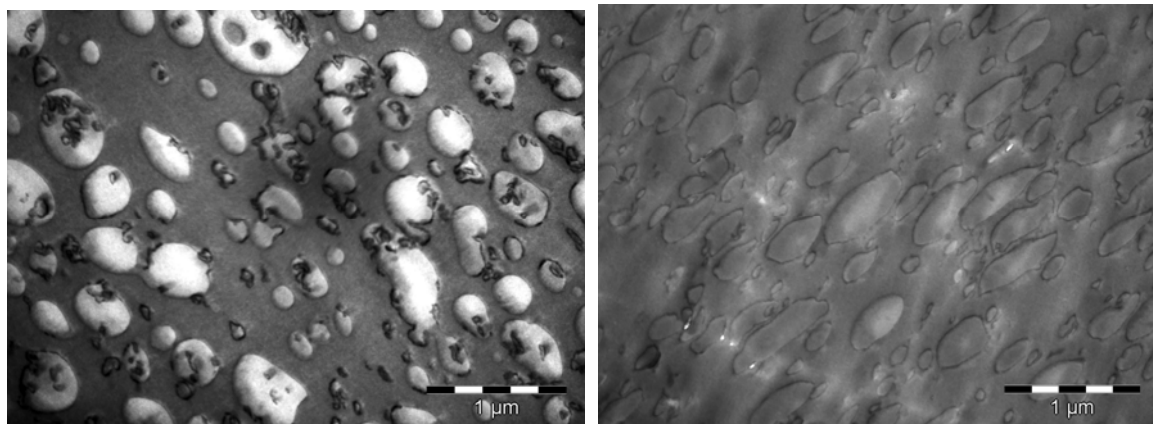


**Fig. 9.** Phase morphology of (PPE/PS)/SAN/SBM blends as a function of the processing conditions. (a) One-step processing, simultaneous compounding of all four components. (b) Two-step processing, pre-blending of (PPE/PS)/SAN and subsequent compatibilization (dark phase: PPE/PS, bright phase: SAN, the polybutadiene of the SBM triblock appears as black phase).

## Conclusions

The present study demonstrates the potential of selective blending for systematically adjusting the phase morphology of immiscible blends. Using immiscible PPE/SAN blends as a reference system, we were able to control the microstructure via blending with PS. The selective miscibility between PS and PPE allowed to adjust the shear viscosity of the high viscous PPE phase, as one of the most relevant factors for the blend morphology. Moreover, a ternary phase diagram of (PPE/PS)/SAN blends were established, highlighting the influence of blend composition and shear-rate on the phase morphology development and co-continuity.

Finally, first steps towards compatibilization of an optimised (PPE/PS)/SAN blend by SBM triblock terpolymers were demonstrated. Nanostructure formation at the interface was observed as a result of the successful compatibilization, while the desired

continuity of the PPE/PS phase was still ensured. It is expected that such quaternary systems reveal excellent mechanical and thermal properties.

In the view of the results, pathways for controlling the micro- and nanostructure of PPE/SAN blends are derived. Nevertheless, the study is not only valid for the present blend system, but for the systematic development of complex, multiphase polymer blends in general.

## Experimental

Unmodified poly(2,6-dimethyl-1,4-phenylene ether) (PPE, grade PX100F, Mitsubishi Engineering Plastics Europe, Düsseldorf) and commercially available poly(styrene-co-acrylonitrile) (SAN, grade VLL 19100, BASF AG, Ludwigshafen) as well as polystyrene (PS, grade 145D, BASF AG, Ludwigshafen) were used for the melt-blending. Due to the acrylonitrile content of 19 wt%, PPE and SAN show immiscibility over the complete compositional range [37]. Symmetric polystyrene-*b*-polybutadiene-*b*-poly(methyl methacrylate) triblock terpolymers (SBM) with a narrow molecular weight distribution ( $M_w/M_n=1.02$ ) were synthesized by anionic polymerization as described previously [3]. The weight content of the respective blocks was 0.33 for PS, 0.34 for PB, and 0.33 for PMMA, the overall number-average molecular weight of SBM was 94 kg/mol. Irganox 1010 and Irgafos 168 (Ciba AG, Basel) were used as stabilisers.

Melt-blending of all materials was performed using a co-rotating twin-screw extruder (Brabender DSE 20/40) with a screw diameter of 20 mm and a length-to-diameter ratio of 29.5. Prior to melt processing, PPE, SAN, and PS were vacuum-dried at 80 °C for at least 12 hours. Subsequently, the materials were dry-blended and fed into the extruder via volumetric feeding. Due to the particular screw setup and the selected processing conditions (screw speed 50 rpm), the mean residence and the melt temperature were 5 min and 260 °C. Subsequently, the melt strand was water-quenched and chopped into pellets.

Besides ternary (PPE/PS)/SAN blends, binary PPE/PS blends and compatibilized, quaternary blends of (PPE/PS)/SAN/SBM were processed. For (PPE/PS)/SAN blends, the content of SAN was fixed at 40 wt%, while the ratio between PPE and PS was varied. Furthermore, as reference systems for the theoretical calculations, miscible PPE/PS blends were processed over the complete compositional range in steps of 25 wt%. Finally, compatibilized (PPE/PS)/SAN/SBM blend systems were processed via two procedures: (i) all four components were fed in the twin-screw extruder and melt-blended; (ii) as a first step, (PPE/PS)/SAN blends were processed to obtain pellets and, as a second step, melt-blended with SBM. All blend compositions are summarised in Fig. 1 and Table 1. It should be noted that 0.1 wt % stabilisers were added in order to prevent thermal degradation (two parts Irganox 1010, one part Irgafos 168).

The shear rheological properties of SAN, PPE and PPE/PS blends were investigated by oscillatory parallel-plate rheometry using a Rheometric Scientific SR 200. For the tests, compression-moulded plates with a diameter of 25 mm and a thickness of 1 mm were used. Prior to the measurement, the specimens were dried under vacuum at 80 °C for at least 4 h. A nitrogen atmosphere during testing was used to prevent oxidative degradation of the sample. Constant stress measurements were performed at different temperature within the viscoelastic regime over a frequency range from 0.01 to 500 rad/s. In order to evaluate the materials characteristics, the complex

viscosity,  $\eta^*$ , the storage modulus, G' and the loss modulus, G'', were obtained. All displayed measurements were performed at 260°C.

**Table 1.** Composition of investigated blend systems.

| Blend no. | Blend name              | wt% PPE/PS | wt% PPE | wt% PS | wt% SAN | PPE/PS ratio |
|-----------|-------------------------|------------|---------|--------|---------|--------------|
| 1         | Binary basic blend 1    | 100        | 75      | 25     | 0       | 75/25        |
| 2         | Binary basic blend 2    | 100        | 50      | 50     | 0       | 50/50        |
| 3         | Binary basic blend 3    | 100        | 25      | 75     | 0       | 25/75        |
| 4         | Original blend          | 60         | 60      | 0      | 40      | 100/0        |
| 5         | Ternary basic blend 1   | 60         | 45      | 15     | 40      | 75/25        |
| 6         | Additional blend 1      | 60         | 36      | 24     | 40      | 60/40        |
| 7         | Ternary basic blend 2   | 60         | 30      | 30     | 40      | 50/50        |
| 8         | Additional blend 2      | 60         | 24      | 36     | 40      | 40/60        |
| 9         | Ternary basic blend 3   | 60         | 15      | 45     | 40      | 25/75        |
| 10        | Optimized ternary blend | 70         | 52.5    | 17.5   | 30      | 75/25        |

For TEM investigation, extruded pellets were cut in perpendicular to the extrusion direction at room temperature using an ultra-microtome (Reichert-Jung Ultracut E microtome). A Zeiss 902 TEM was used at an acceleration voltage of 80 kV to observe micrographs of the blends morphology. Ultrathin sections of 40 nm thickness were stained using OsO<sub>4</sub> and RuO<sub>4</sub> according to a procedure outlined recently [3]. Due to the particular conditions, SAN appeared bright, while PPE and its blends with PS form the dark phase in bright field transmission electron microscopy. In addition, for blends compatibilized by SBM, the polybutadiene of the triblock terpolymers can be detected as black phase. Representative TEM micrographs of all blends are shown here, and the characteristics of each blend verified by at least ten further micrographs.

The blend phase morphology was quantitatively accessed by evaluation of TEM micrographs via image analyzing software (ImageJ). Besides the particle size, the co-continuity of the blend system was expressed by the so-called form factor, F, which is based on the perimeter, P, and the area, A, of each particle (Eq. 5). In addition, the co-continuity of the system was evaluated based on the form factors and the area of the individual particles (Eq. 6).

### Acknowledgements

The authors thank the German Science Foundation (Deutsche Forschungsgemeinschaft, DFG) for funding of this work under SFB 481 (project A10). We are grateful to Dr. M. Weber (BASF AG, Ludwigshafen) for providing the neat polymers SAN and PS, respectively, and to C. Kunert (Polymer Engineering and SFB 481, Z4) for the transmission electron microscopic investigations.

### References

- [1] Paul, D.R.; Bucknall C.B. *Polymer Blends* **2000**, John Wiley & Sons, INC., New York.

- [2] Utracki, L. A. *Polymer Alloys and Blends*, **1989**, 1. Print, München, Hanser Verlag.
- [3] Ruckdäschel, H.; Sandler, J. K. W.; Altstädt, V.; Rettig, C.; Schmalz, H.; Abetz, V.; Müller, A. H. E. *Polymer* **2006**, 47, 2772.
- [4] Ruckdäschel, H.; Sandler, J. K. W.; Altstädt, V.; Schmalz, H.; Abetz, V.; Müller, A. H. E. *Polymer* **2007**, 48, 2700.
- [5] Auschra, C.; Stadler, R. *Macromolecules* **1993**, 26, 6364.
- [6] Pötschke, P.; Paul, D. R. *J. Macromol. Sci. Pol. R.* **2003**, C43, 87.
- [7] Steinmann, S.; Gronski, W.; Friedrich, C. *Polymer* **2001**, 42, 6619.
- [8] Veenstra, H.; van Lent, B. J. J.; van Dam, J.; de Boer, A. P. *Polymer* **1999**, 40, 6661.
- [9] Veenstra, H.; Norder, B.; van Dam, J.; de Boer, B. P. *Polymer* **1999**, 40, 5223.
- [10] Marin, N.; Favis, B. D. *Polymer* **2002**, 43, 4723.
- [11] Prochazka, F.; Dima, R.; Majeste, J. C.; Carrot, C. *E-Polymers* **2003**.
- [12] Willemse, R. C.; de Boer, A. P.; van Dam, J.; Gotsis, A. D. *Polymer* **1999**, 40, 827.
- [13] Willemse, R. C.; de Boer, A. P.; van Dam, J.; Gotsis, A. D. *Polymer* **1998**, 39, 5879
- [14] Mekhilef, N.; Verhoogt, H. *Polymer* **1996**, 37, 4069.
- [15] Steinmann, S.; Gronski, W.; Friedrich, C. *Rheol. Acta* **2002**, 41, 77.
- [16] He, J. S.; Bu, W. S.; Zeng, J. J. *Polymer* **1997**, 38, 6347.
- [17] Joseph, S.; Rutkowska, M.; Jastrzebska, M.; Janik, H.; Haponiuk, J. T.; Thomas, S. *J. Appl. Polym. Sci.* **2003**, 89, 3700.
- [18] Potschke, P., Paul, D. R. *Macromol. Symp.* **2003**, 198, 69.
- [19] Cook, W. D.; Zhang, T.; Moad, G.; VanDeipen, G.; Cser, F.; Fox, B.; Oshea, M. *J. App. Polym. Sci.* **1996**, 62, 1699.
- [20] Cook, W. D.; Moad, G.; Fox, B.; VanDeipen, G.; Zhang, T.; Cser, F.; McCarthy, L. *J. App. Polym. Sci.* **1996**, 62, 1709.
- [21] Kolarik, J.; Lednický, F.; Locati, G.; Fambri, L. *Polym. Eng. Sci.* **1997**, 37, 128.
- [22] Quintens, D.; Groeninckx, G.; Guest, M.; Aerts, L. *Polym. Eng. Sci.* **1991**, 31, 1207.
- [23] Chun, B. C.; Gibala, R. *Polym. Eng. Sci.* **1996**, 36, 744.
- [24] Harrats, C.; Thomas, S.; Groeninckx, G. *Micro- and Nanostructured Multiphase Polymer Blends*; Taylor&Francis Group, LLC, 2006.
- [25] Potente, H.; Bastian, M.; Bergemann, K.; Senge, M.; Scheel, G.; Winkelmann, T. *Polym. Eng. Sci.* **2001**, 41, 222.
- [26] Everaert, V.; Aerts, L.; Groeninckx, G. *Polymer* **1999**, 40, 6627.
- [27] Tol, R. T.; Groeninckx, G.; Vinckier, I.; Moldenaers, P.; Mewis, J. *Polymer* **2004**, 45, 2587.
- [28] Lovera, D.; Ruckdaschel, H.; Goldel, A.; Behrendt, N.; Frese, T.; Sandler, J. K. W.; Altstadt, V.; Giesa, R.; Schmidt, H. W. *Eur. Polym. J.* **2007**, 43, 1195.
- [29] A. F. Yee; J. *Polym. Eng. Sci.* **1977**, 17, 213.
- [30] Kleiner, L. W.; Karasz, F. E.; Macknight, W. J. *Polym. Eng. Sci.*, **1979**, 19, 519.
- [31] Everaert, V.; Aerts, L.; Groeninckx, G. *Polymer* **1999**, 40, 6627.
- [32] Schramm, G. *A Practical Approach to Rheology and Rheometry* **1994**, Karlsruhe: Gebrueder HAAKE GmbH, 1994.
- [33] Miles, I. S.; Zurek A. *Polym. Eng. Sci.* **1988**, 28, 796.
- [34] Utracki L.A. *J. Rheol.* **1991**, 35, 1615.
- [35] Sundararaj, U.; Macosko, C. W. *Polym. Eng. Sci.* **1996**, 36, 1769.
- [36] Potente H.; Bastian M. *Polym. Eng. Sci.* **2000**, 40, 727.
- [37] Suess, M.; Kressler, J.; Kammer, H. W. *Polymer* **1987**, 28, 957.

- [38] Steinmann, S.; Gronski, W.; Friedrich, C. *Polymer* **2001**, 42, 6619.
- [39] Milner, S.T.; Xi, H.W. *J. Rheol.*, **1996**, 40, 663.
- [40] Kopczynska, A.; Ehrenstein, G.W. *J. Mater. Ed.* **2007**, 29, 325